Zitierweise: *Angew. Chem. Int. Ed.* **2024**, *63*, e202401743
doi.org/10.1002/anie.202401743

Propellants

Controlled Release of Diborane from Alkali Metal Borohydride using Ionic Liquid-Based Lewis Acids

*Ashvin Kumar Vasudevan[+], Yujie Wang[+], Prithwish Biswas, Keren Shi, and Michael R. Zachariah**

Abstract: Alkali metal borohydrides present a rich source of energy dense materials of boron and hydrogen, however their potential in propellants has been hitherto untapped. Potassium borohydride is a promising fuel with high gravimetric energy density and relatively low sensitivity to air and moisture. Problems arise due to the dehydrogenation of the borohydride on heating with minimal energy release. Common methods to extract both boron and hydrogen by means of borane species involve direct reaction of boron trifluoride species with alkali borohydrides. However, these methods face storage and safety issues due to rapid release of diborane on mixing the reactants. We propose a method of diborane release through controlled release of boron trifluoride by means of a tetrafluoroborate based ionic liquid. The trifluoride is released from the ionic liquid at elevated temperatures and enables safe mixture of the reactants at room temperature. It was found that the reaction between borohydride and boron trifluoride proceeds well above room temperature with potassium borohydride releasing diborane and potassium fluoride. The reaction pathway shows a primary reaction releasing diborane and potassium fluoride and a second less energy efficient step leading to the formation of potassium tetrafluoroborate. A 3D printed propellant formulation was also tested.

Introduction

Complex hydrides with light weight metals provide a safe source of hydrogen with manageable storage requirements when compared to liquid cryogenic sources. Metal hydrides are potential candidates as additives for solid propellants as they offer higher regression rates, specific impulse and minimal metal agglomeration. The performance of solid propellants was found to improve due to increases in the gravimetric specific impulse.[1–4] Issues arise however, due to aging and stability concerns and limited compatibility with the oxidizers and binders added in common propellants.[5] Other concerns include susceptibility to dehydrogenation in the presence of moisture.[6]

Boranes in the form of borohydrides have been considered primarily as hydrogen storage materials due to their high gravimetric/volumetric hydrogen storage capacities.[7] Sodium borohydride has found utility in hydrogen storage and production, direct fuel cells, reduction reactions, synthesis and surface modifications.[8–15] Problems arise due to the moisture sensitivity of borohydrides during storage. Potassium borohydride offers an equally efficient source of hydrogen as sodium but with higher stability. However, it has not been studied with as much detail and has mostly been restricted to hydrogen production applications.[16,17] The strong reduction efficiency of potassium borohydride enables its application as a catalyst for organic and metal reductions.[18,19]

For rocket propellant applications, sodium borohydride has been used as a non-toxic hypergolic propellant additive with hydrogen peroxide. These mixtures require careful storage conditions and separation. Moreover, the primary reaction products were found to be sodium metaborate and metaboric acid indicating that the energy potential from boron was not fully realized.[20,21] The incentive to use both elements with high energy density has led to consideration of ammonia borane and other complex amine-based borohydrides.[22,23] Recently, successful attempts have been made to harvest energy from both boron and hydrogen in ammonia borane composites with the help of ammonium perchlorate and polymeric carbonyl groups.[24,25]

Borohydrides have been used as safe solid sources of diborane in rocket propellants, as reducing agents or in semiconductor fabrication. The common methods include reactions with boron trifluoride etherate or inorganic acids. A strong acid is required, after which the diborane released is separated and stored for later use.[26–29] However, diborane is extremely unstable and has a propensity to form higher boranes and degrade while being stored. Highly porous materials are required for efficient storage.[30] Air breathing propulsion utilizes surrounding air as the oxidizer for combustion of the fuel carried onboard.[31] Diborane when released, auto ignites in air at about 40 °C which would make it a good candidate for air breathing propulsion applications.[32]

The metal-boron bond requires a strong Lewis acid such as boron trifluoride to cleave and release diborane. The aim of the current work is to provide an effective method to release diborane from alkali borohydrides thermally while

[*] A. Kumar Vasudevan,[+] Y. Wang,[+] P. Biswas, K. Shi, M. R. Zachariah
Department of Chemical and Environmental engineering
University of California, Riverside
900 University avenue, Riverside, CA—92521
E-mail: mrz@engr.ucr.edu

[+] These authors contributed equally

retaining their stability at room temperature. For this purpose, 1-ethyl-3-methylimidazolium tetrafluoroborate, a source of boron trifluoride, was employed. The Lewis acid, boron trifluoride, is released only on heating, hence the mixture of borohydride and ionic liquid remains stable at room temperature. Since potassium borohydride is less sensitive to moisture, it was chosen over sodium borohydride for the experiments. High heating rate time-of-flight mass spectrometry (TOFMS) measurements revealed the release temperature of diborane from the potassium borohydride-ionic liquid mixture to be around 290 °C. The released diborane spontaneously ignited with atmospheric oxygen and required no additional oxidizer. This system provides a method for controlled release of diborane for air-breathing applications.

Results and Discussion

Reaction Products Under High Heating Rate Measurements (~10^5 K/s)

The gaseous species evolved during the reaction of potassium borohydride and the ionic liquid were probed at a heating rate of 10^5 K/s. Figure 1a shows the decomposition of neat potassium borohydride (KBH_4) and 1-ethyl-3-methylimidazolium tetrafluoroborate ($EMIMBF_4$) as well as KBH_4 and $EMIMBF_4$ mixtures with different ratios (25–75 wt %, 45–55 wt %, and 60–40 wt %). KBH_4-$EMIMBF_4$ 45–55 wt % mixture is believed to be stoichiometric, which will be discussed in detail in the following sections. Release of hydrogen and potassium (m/z = 39), which is believed to be from the ionization of potassium hydride, are seen with neat KBH_4, but no diborane is released as expected. $EMIMBF_4$ decomposes to its corresponding ions EMIM (m/z = 111) and BF_3 (BF_2, m/z = 49). Methyl imidazole (m/z = 82), a fragment of the imidazole (m/z = 42), as well as small amounts of ethyl imidazole (m/z = 96) and imidazole (m/z = 69), are also observed.

When mixed, however, clear evidence of the diborane (m/z = 28) release with an absence of potassium/potassium hydride peaks from neat KBH_4 can be seen. Peaks corresponding to the decomposition of $EMIMBF_4$ are observed in all weight proportions of the mixture.

The peak corresponding to potassium is observed only in the mixture of 60–40 wt % of KBH_4-$EMIMBF_4$, indicating an excess of KBH_4 at this ratio. The m/z = 28 peak could also be due to the C_2H_4 fragments released from the ionic liquid. Hence, for the mixture, there are three species contributing to the intensities of the m/z = 28 peak namely N_2, C_2H_4 and B_2H_6. It is noteworthy that N_2 is always present in the TOFMS chamber even under high vacuum (~10^{-9} atm), and N_2 only shows a m/z = 28 peak. Both C_2H_4 and B_2H_6 are expected to produce fragments in addition to this peak at m/z = 26, 27, and 29. However, the green flame observed from the ignition and combustion tests is attributed to the molecular emission from BO_2,[33,34] which demonstrates B_2H_6 is released from the reaction. This will be discussed in more detail in the following sections.

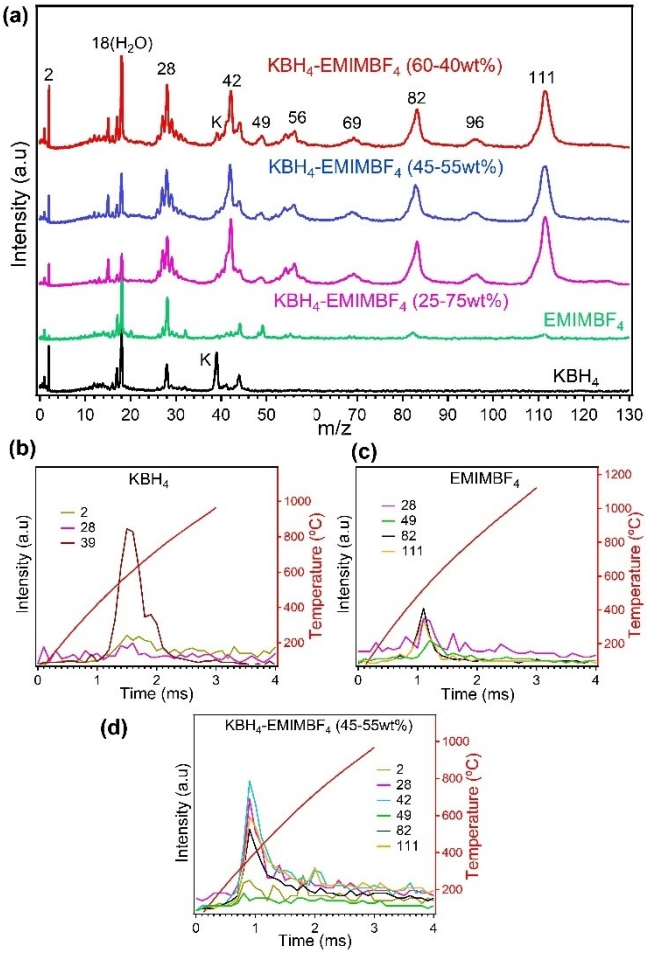

Figure 1. a) T-Jump TOFMS spectra shows the diborane release along with the decomposition products of neat $EMIMBF_4$, KBH_4, and mixtures at various ratios. Different species released over time and corresponding heating profile of neat KBH_4 (b), neat $EMIMBF_4$ (c), and stoichiometric mixture of KBH_4 and $EMIMBF_4$ (d).

The temporal evolution of the species for the individual components shown in Figure 1(b) and (c) demonstrates that neat KBH_4 decomposes at ~470 °C and neat $EMIMBF_4$ decomposes at ~400 °C. However, for the 45–55 wt % mixture shown in Figure 1(d), the species release temperature of $EMIMBF_4$ is observed to be as low as ~290 °C, indicating a faster decomposition in the presence of KBH_4. Boron trifluoride (BF_3) fragment (m/z = 49) is observed for measurements at each mass ratio.

Thermal Behaviour Under Slow Heating Rate (10 K/min)

Thermogravimetric analysis of neat KBH_4, neat $EMIMBF_4$, and KBH_4-$EMIMBF_4$ (45–55 wt %) is shown in Figures S2 and 2 respectively. For the sample with 45–55 wt % of KBH_4-$EMIMBF_4$, there are two mass loss steps observed which can be attributed to the reaction. The initial mass loss step between 120–280 °C was taken as the primary mass loss step where the majority of the diborane is released as

observed by TOFMS measurements (Figure 1(d)). An additional mass loss step is observed between 450–550 °C. This mass loss step was later found to be due to decomposition of $K_2B_{12}H_{12}$ (Figure 4). The mixture with a 60–40 wt % shows a prominent mass loss step around 600 °C in addition to the primary mass loss step, which is consistent with observed neat KBH_4 mass loss (Figure S2). This mass loss indicates that there is excess KBH_4 which decomposes at high temperature. Similar to neat KBH_4 mass spectrometry data, potassium peak (m/z = 39) is observed in the TOFMS data (Figure 1(a)) for this mixture. The mixture of 25–75 wt % shows a second mass loss step between 280–400 °C which indicates decomposition of excess ionic liquid (Figure S2). The sample of 45–55 wt % is taken as the stoichiometric condition for the reaction of KBH_4 and BF_3 from the ionic liquid.

This mass ratio corresponds to the stoichiometric condition for formation of KF rather than KBF_4 from the mixture as shown in the following Reaction (i).

$$3KBH_4 + BF_3 \rightarrow 2B_2H_6 + 3KF \quad \text{(i)}$$

In this scenario, the boron is efficiently converted to diborane without the formation of KBF_4.

Characterization of Condensed-Phase Reaction Products

XRD was used to characterize the condensed phase products around the featured temperatures identified by TGA for the stoichiometric mixture (45–55 wt %). As shown in Figure 2, the primary mass loss begins at ~120 °C and ends at ~280 °C. The mixture was heated to three temperatures (120 °C, 200 °C, and 300 °C) to reflect three stages of the reaction (at the beginning, during, and at the end. The expected products of the reaction of KBH_4 and BF_3 are potassium tetrafluoroborate (KBF_4) and potassium fluoride (KF). XRD patterns of the stoichiometric mixture (45–55 wt %) show mostly KBH_4 peaks with almost no KBF_4 or KF as seen in Figure 3 . Since the products are believed to be moisture sensitive, the sample was heated in a furnace filled with argon, and then packed using a polyamide film for XRD measurements. However, we note that exposure to air cannot be eliminated during sample transfer. XRD measurements in argon show peaks for KBF_4 but no KF. $KF{\cdot}2H_2O$ is likely formed as it is more stable than KF at room temperature[35] with absorption of moisture leading to loss of crystallinity. KBF_4, while also being moisture sensitive, is sufficiently stable to be detected in XRD after exposure to moisture during sample transfer. Any KBF_4 formed in the presence of air at 300 °C, appears to have degraded with no peaks observed in XRD measurements.

Nuclear Magnetic Resonance (NMR) Spectra

B^{11} nuclear magnetic resonance spectra, shown in Figure 4, were taken for samples heated in argon and loaded onto a zirconia rotor for solid state magic angle spinning measurements. As received KBH_4 powder (−38.0 ppm) is taken as a reference for the measurement.[36] Once mixed with the ionic liquid we observe BH_4^- along with the BF_4 from the ionic liquid at −2.5 ppm. On heating to 200 °C, the peak intensity of BF_4 decreases, and only the BH_4^- peak is visible. The consumption of the BF_4 is indicative of the reaction which begins around 120 °C and ends at 280 °C as observed by the primary mass loss in the TGA. On further heating to 300 °C, a BF_4 peak attributed to KBF_4 is observed. This KBF_4 is likely produced by a slow reaction of KBH_4 and BF_3. BH_4^- is completely consumed above 450 °C with a new peak observed, which appears to correspond to BF_3 adsorbed on metal oxide surfaces.[37]

The NMR spectrum observed at 550 °C shows a peak around −15 ppm, which is attributed to $K_2B_{12}H_{12}$.[38–40] The formation of $B_{12}H_{12}^{2-}$ involves dehydrogenation of KBH_4 to KB_3H_8 and eventually to $K_2B_{12}H_{12}$ in the presence of iodine

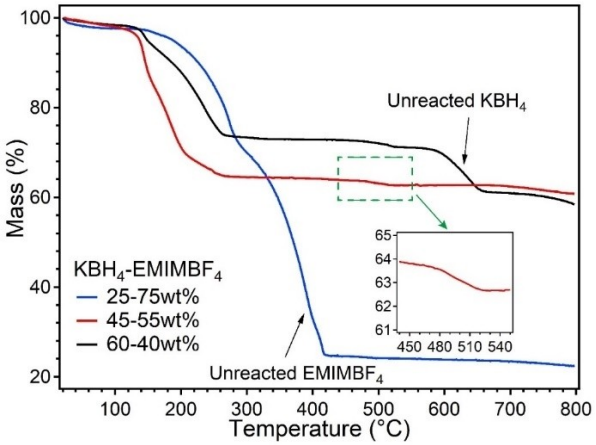

Figure 2. Decomposition steps observed with different weight proportions of KBH_4 to $EMIMBF_4$.

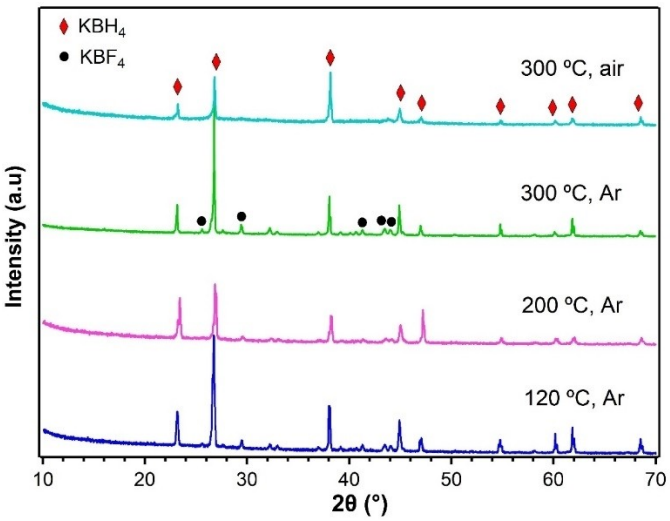

Figure 3. XRD patterns of stoichiometric mixtures of KBH_4-$EMIMBF_4$ (45–55 wt %) heated in air and argon at different temperatures.

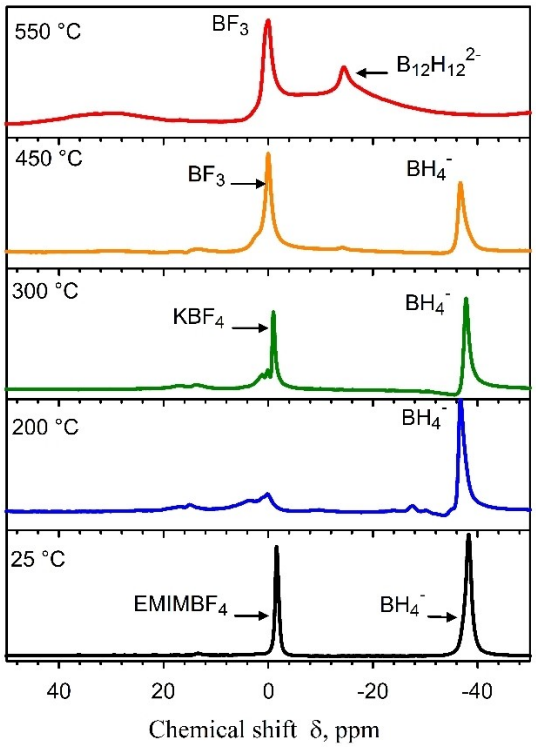

Figure 4. B^{11} NMR spectra for KBH_4-$EMIMBF_4$ (45–55 wt%) heated at different temperatures.

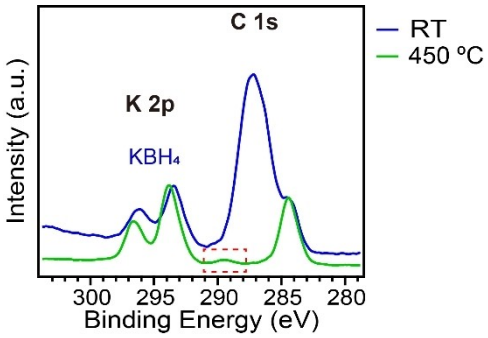

Figure 5. XPS spectra of stoichiometric mixture of KBH_4-$EMIMBF_4$ (45–55 wt%) in vacuum at room temperature (RT) and heated to 450 °C showing C 1s and K 2p binding energies. The new peak (inside the dashed box) observed at 450 °C in the C 1s spectrum at 289 eV was attributed to C–F bond formation.

or through reaction of KBH_4 with diborane, according to ref..[40] Both these mechanisms involve formation of $B_{10}H_{10}^{2-}$ and $B_{11}H_{14}^{-}$ species through gradual dehydrogenation.

In the observed NMR spectra, there are no peaks which can be attributed to KB_3H_8, $B_{10}H_{10}^{2-}$ or $B_{11}H_{14}^{-}$. The peak observed around 0 ppm does not correspond to any borane species. The observed $K_2B_{12}H_{12}$ is presumably formed through a fast dehydrogenation reaction since the residual KBH_4 is converted to $K_2B_{12}H_{12}$ between 450–550 °C with none of the expected intermediates observed. The formation of $K_2B_{12}H_{12}$ is likely due to the reaction of unreacted KBH_4 and the KBF_4 formed as shown in ref..[41] KBF_4 decomposes at temperatures higher than 530 °C producing KF and BF_3.[42] The NMR peak at 0 ppm at 450–550 °C corresponds to BF_3 adsorbed on metal oxide surfaces,[37] indicating faster decomposition than expected of neat KBF_4 . Further study is required to verify adsorption of BF_3 on the KBH_4 surface and release at high temperatures through decomposition of KBF_4.

The $K_2B_{12}H_{12}$ formed is expected to decompose to form $K_2B_{12}H_{12-x}$ species which eventually forms polymers of the order $(K_2B_{12}H_z)_n$.[43] The slow TGA mass loss observed > 550 °C for the stoichiometric mixture (45–55 wt %), as shown in Figure 2, is attributed to the decomposition of $K_2B_{12}H_{12}$.

X-ray Photoelectron Spectra (XPS)

Figure 5 shows XPS spectra for C 1s and K 2p of KBH_4-$EMIMBF_4$ (45–55 wt %) at room temperature and after heating to 450 °C. At room temperature, K 2p splitting (293 and 296 eV) are attributed to KBH_4.[44] The C 1s has a broad peak between 289 and 285 eV with a shoulder at 285 eV, is attributed to carbons in EMIM,[45] and the shoulder at 285 eV is reported to be the total binding energies of CH_3 in the $EMIMBF_4$ and the interstitial carbon(C–C) peak at 284.8 eV. At 450 °C, the peaks linked to the carbons in EMIM dissappear entirely due to decomposition/reaction and new peak is observed ~289 eV, the closest match of which is the C–F bond (Figure 5).[47] K 2p peaks are observed to room temperature KBH_4 with a slight shift of 0.2 eV. K 2p binding energies of KF are very close to those of KBH_4.[48] However, the expected F 1s peak for KF at 684 eV[46] is not present. KF can participate in nucleophilic attacks on ionic liquids, amines and other compounds[50] so fluorination of EMIM is a plausible reason for the absence of the KF F 1s peak.

Analysis of the XPS spectra of F 1s and B 1s (Figure S4) demonstrates that BF_3 is produced from the reaction and adsorbed on the sample surface (more details can be found in the Supporting Information Figure S4). This is consistent with the NMR data at 450 °C.

Ignition and Combustion Characteristics

Figure 6 (a) and (b) show MW initiated and wire ignition of the prepared KBH_4-$EMIMBF_4$ mixture, respectively, with the characteristic green flame observed away from the sample due to molecular emission of BO_2 from the combustion of diborane in air.[33,34] Figure 6 (c) shows the propagation of 3D printed 90 % loading composites with a PMMA binder. Similar to the observation from the ignition tests, the diborane is found to burn away from the burning surface, due to gas phase reaction with air. The molten surface is found to emit radiation that is believed to be from potassium.[51] There is an orange flame observed closer to the stick surface. This could be caused by combustion of potassium hydride (KH) formed through incomplete decomposition of KBH_4 and/or the combustion of organic fragments from the decomposition of $EMIMBF_4$.

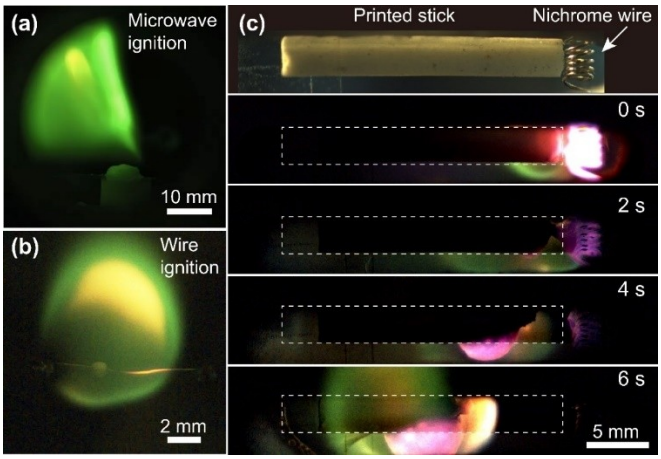

Figure 6. (a) Microwave ignition and (b) T-Jump ignition of the reactant mixture of KBH_4-$EMIMBF_4$ at the stoichiometric condition (45–55 wt%). (c) Snapshots of combustion process of the 3D printed composites containing stoichiometric mass ratio of KBH_4 to $EMIMBF_4$ with 10 wt % of PMMA binder.

This orange flame is also observed through T-Jump and microwave ignition measurements (Figure 6 (a) and (b)).

Proposed Reaction Mechanism

Early literature work[28] describes reactions conducted in liquid phase between $NaBH_4$ and BF_3 using solvents such as tetrahydrofuran (THF) and diglyme to produce diborane. Borane formed was expected to form an intermediate with sodium borohydride in solution[28] and subsequently release diborane and potassium tetrafluoroborate. Hence, preliminary tests with potassium borohydride were carried out with stoichiometric ratios corresponding to the following Reaction (ii). This stoichiometric condition corresponds to the 25–75 wt % KBH_4-$EMIMBF_4$ shown in Figure 2.

$$3KBH_4 + 4BF_3 \rightarrow 2B_2H_6 + 3KBF_4 \quad \text{(ii)}$$

Evidence of neat EMIMBF4 was found through these tests and this reaction was not considered stoichiometric moving forward.

As observed from our TGA measurements (Figure 2), decomposition of unreacted $EMIMBF_4$ and KBH_4 are observed for weight proportions above and below the 45–55 wt % of reactants respectively. The following reaction is believed to take place at 45–55 wt % as the ratio confirms to its stoichiometry (Reaction i)..

The formation of KF at its stoichiometric condition indicates complete conversion of boron and hydrogen from the reactants to diborane (Reaction (i)). While XRD and XPS measurements of samples do not show the presence of KF, XRD measurements for reacted mixtures of $NaBH_4$ and $EMIMBF_4$ show strong NaF peaks as seen in Figure 7. The evolved species and observed mass loss observed from TOFMS and TGA data respectively, show a similar reaction mechanism for the Na and K based systems.

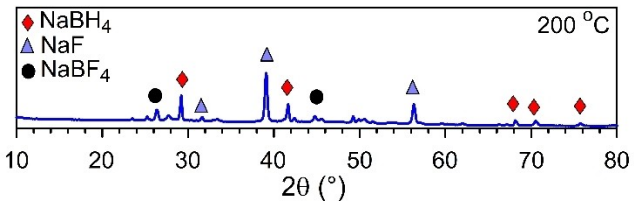

Figure 7. X ray diffraction pattern of stoichiometric weight ratio of $NaBH_4$ and $EMIMBF_4$.

While the common reaction pathway with BF_3 is expected to form KBF_4 as observed with liquid phase synthesis,[28] TGA analysis indicates the formation of KF since there are no decompositions of unreacted reactants observed for its stoichiometric condition (KBH_4-$EMIMBF_4$ 45–55 wt %). At temperatures around 150 °C, boron trifluoride reacts with sodium borohydride to form difluoroborane (HBF_2).[52] Experimental evidence[52] outlines hydrogen removal from $NaBH_4$ to reduce BF_3 to HBF_2.

The decomposition mechanism for sodium and potassium borohydrides is of the form

$$M(BH_4) \rightarrow MH + B + 1.5H_2$$

The heats of formation, heats of desorption (around 90 kJ/mol) and hydrogen capacities are very similar for both borohydrides as shown in ref..[53] Hence, one should reasonably expect the same mechanism to be valid for KBH_4 forming HBF_2 from KBH_4. KBH_4 performs better than $NaBH_4$ in our experimental conditions by virtue of its lower moisture sensitivity. The HBF_2 can subsequently form boron trifluoride as shown in[54] releasing some diborane. A tentative mechanism is depicted in Figure 8.

The BF_3 formed reacts with KBH_4 to further reduce to HBF_2 with diborane released at each step. The primary and secondary pathways are shown in Figure 8. The total mass loss observed for the individual mass losses from the TGA were calculated in terms of moles of KBH_4 occurring in each reaction. As seen in the TGA (Figure 2), 80–90 % of the total mass loss occurs between 120–280 °C producing KF and diborane. A gradual mass loss occurs till 350 °C, possibly to form KBF_4 and diborane (Reaction 2) as observed from the NMR data (Figure 4). The KBF_4 formed further reacts with KBH_4 to form potassium dodecaborane($K_2B_{12}H_{12}$). Here, the gas phase products were assumed to be B_2H_6 and $EMIMF^-$ in each case to calculate amount of KBH_4 used in each pathway.

Primary Reaction Step

a) Formation of HBF_2 and BH_3 Through Hydrogen Abstraction

Decomposition of HBF_2 to BF_3

$$6HBF_2 \rightarrow 4BF_3 + B_2H_6$$

a) Formation of HBF_2 and BH_3 through hydrogen abstraction

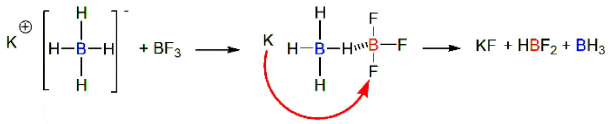

b) Decomposition of HBF_2 to BF_3

$$6HBF_2 \rightarrow 4BF_3 + B_2H_6$$

The global reaction is specified in reaction 1.

Secondary reaction step

c) Slow reaction of KBH_4 with BF_3 forming KBF_4

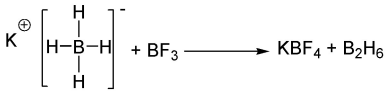

d) Formation of $K_2B_{12}H_{12}$

$$36KBH_4 + 10KBF_4 \rightarrow 3K_2B_{12}H_{12} + 40KF + 10B + 54H_2$$

Figure 8. Formation of KF and KBF_4 through hydrogen abstraction with release of boranes through primary and secondary reactions

The global reaction is specified in reaction 1.

Secondary Reaction Step

c) Slow Reaction of KBH_4 with BF_3 Forming KBF_4

Formation of $K_2B_{12}H_{12}$

$$36KBH_4 + 10KBF_4 \rightarrow 3K_2B_{12}H_{12} + 40KF + 10B + 54H_2$$

Most of the diborane is released in reaction 1 between 120–280 °C as seen in Figure 2. The subsequent mass loss step seen between 470–520 °C is attributed to the formation of $K_2B_{12}H_{12}$ through gradual release of hydrogen as shown in Reaction 4. The $K_2B_{12}H_{12}$ later decomposes slowly to form species of the form $K_2B_{12}H_{12-x}$ and polymerize on further heating to give $(K_2B_{12}H_z)_n$ as shown in ref. [43].

In addition to the formation of $K_2B_{12}H_{12}$, KBF_4 can also decompose to boron trifluoride and potassium fluoride (Reaction 3) as observed by the NMR measurements shown in Figure 4. The boron trifluoride appears to be bound to the KBH_4 surface to some degree.

To summarize, the various reactions taking place in the KBH_4-$EMIMBF_4$ system are:

1) The primary reaction which results in the formation of diborane and potassium fluoride.
$$3KBH_4 + BF_3 \rightarrow 2B_2H_6 + 3KF$$

2) The side reaction with gradual formation of KBF_4.
$$3KBH_4 + 4BF_3 \rightarrow 2B_2H_6 + 3KBF_4$$

3) Decomposition of KBF_4
$$\rightarrow BF_3 + KF$$

4) Formation of $K_2B_{12}H_{12}$
$$36KBH_4 + 10KBF_4 \rightarrow 3K_2B_{12}H_{12} + 40KF + 10B + 54H_2$$

5) Polymerization of $K_2B_{12}H_{12}$

Conclusion

Ionic liquid (1-ethyl-3-methylimidazolium tetrafluoroborate, $EMIMBF_4$) has been employed to serve as a source of BF_3 to facilitate the controllable release of diborane from KBH_4 on heating while maintaining stability at room temperature. Through hydrogen abstraction from KBH_4, an atom efficient pathway to generate KF and diborane occurs through the action of the Lewis acid, BF_3. TGA and TOFMS measurements underline a reaction pathway producing diborane from the mixture of KBH_4 and $EMIMBF_4$ at stoichiometric ratio. Ignition test of this mixture reveals a green flame in the gas phase away from the sample, indicating a gas phase reaction of boron species with air, thereby confirming diborane release. A reaction mechanism is proposed to describe the reaction pathways. Both $NaBH_4$ and KBH_4 are found to follow the same mechanism. Free-standing 90 wt % loading of KBH_4-$EMIMBF_4$ at stoichiometric ratio is prepared for showing the potential application of metal borohydride with ionic liquid as a propulsion formulation. EMIM fragments released are also found to combust in air, indicating two potential air breathing fuel sources in the composite. Further studies are required to test the various other hydrides to investigate if the release temperature of diborane is controllable.

Acknowledgements

This work is supported by the Office of Naval Research.

Conflict of Interest

The authors declare no conflict of interest.

Data Availability Statement

The data that support the findings of this study are available from the corresponding author upon reasonable request.

Keywords: Ionic liquid · Borohydride · Air breathing propellant · Controlled decomposition · Gas phase combustion

[1] B. Sakintuna, F. Lamari-Darkrim, M. Hirscher, *Int. J. Hydrogen Energy* **2007**, *32*, 1121–1140.

[2] M. Devarakonda, K. Brooks, E. Rönnebro, S. Rassat, *Int. J. Hydrogen Energy* **2012**, *37*, 2779–2793.
[3] F. Maggi, G. Gariani, L. Galfetti, L. T. DeLuca, *Int. J. Hydrogen Energy* **2012**, *37*, 1760–1769.
[4] M. L. Chan, C. L. Johnson, in *Proceedings*, **2003**.
[5] L. George, S. K. Saxena, *Int. J. Hydrogen Energy* **2010**, *35*, 5454–5470.
[6] F. A. Cotton, G. Wilkinson, C. A. Murillo, M. Bochmann, *Advanced Inorganic Chemistry*, John Wiley & Sons, **1999**.
[7] L. Schlapbach, A. Züttel, *Nature* **2001**, *414*, 353–8.
[8] H. N. Abdelhamid, *Int. J. Hydrogen Energy* **2021**, *46*, 726–765.
[9] T. Avci Hansu, O. Sahin, A. Caglar, H. Kivrak, *React. Kinet. Mech. Catal.* **2020**, *131*, 661–676.
[10] G. W. Gribble, *Chem. Soc. Rev.* **1998**, *27*, 395–404.
[11] U. T. Khatoon, A. Velidandi, G. V. S. Nageswara Rao, *Mater. Chem. Phys.* **2023**, *294*, 126997.
[12] D. Xu, Y. Zhang, Q. Guo, *Int. J. Hydrogen Energy* **2022**, *47*, 5929–5946.
[13] U. B. Demirci, P. Miele, *Energy Environ. Sci.* **2009**, *2*, 627–637.
[14] P. Dai, Y. Yao, E. Hu, D. Xu, Z. Li, C. Wang, *Appl. Surf. Sci.* **2021**, *546*, 149128.
[15] S. Sun, H. Yu, L. Li, X. Yu, X. Zhang, Z. Lu, X. Yang, *Metals* **2022**, *12*, DOI 10.3390/met12071059.
[16] A. Balbay, C. Saka, *Int. J. Hydrogen Energy* **2018**, *43*, 21299–21306.
[17] M. Salih Keskin, Ö. Şahin, S. Horoz, *J. Aust. Ceram. Soc.* **2022**, *58*, 973–979.
[18] Q. Zhang, Z. Yang, B. Ding, X. Lan, Y. Guo, *Transactions of Nonferrous Metals Society of China - TRANS NONFERROUS METAL SOC CH* **2010**, *20*, DOI 10.1016/S1003-6326(10)-60047-7.
[19] Y. Liu, B. Liu, A. Guo, Z. Dong, S. Jin, Y. Lu, *Molecules* **2011**, *16*, 3563–3568.
[20] H. Kang, J. Won, S. W. Baek, S. Kwon, *Combust. Flame* **2017**, *181*, 149–156.
[21] D. A. Castaneda, B. Natan, *Fuel* **2022**, *316*, 123432.
[22] M. J. Baier, A. J. McDonald, K. A. Clements, C. S. Goldenstein, S. F. Son, *Proc. Combust. Inst.* **2021**, *38*, 4433–4440.
[23] X. Huang, S. Li, X. Zheng, S. Yang, Y. Guo, *Energy Fuels* **2016**, *30*, 1383–1389.
[24] P. Biswas, P. Ghildiyal, H. Kwon, H. Wang, Z. Alibay, F. Xu, Y. Wang, B. M. Wong, M. R. Zachariah, *J. Phys. Chem. C* **2022**, *126*, 48–57.
[25] P. Biswas, Y. Wang, S. Herrera, P. Ghildiyal, M. R. Zachariah, *Chem. Mater.* **2023**, *35*, 954–963.
[26] R. M. Adams, in *BORAX TO BORANES*, American Chemical Society, **1961**, pp. 60–68.
[27] H. D. Batha, E. D. Whitney, T. L. Heying, J. P. Faust, S. Papetti, *J. Appl. Chem.* **1962**, *12*, 478–481.
[28] J. V. B. Kanth, H. C. Brown, *Inorg. Chem.* **2000**, *39*, 1795–1802.
[29] H. G. Weiss, I. Shapiro, *J. Am. Chem. Soc.* **1959**, *81*, 6167–6168.
[30] N. B. Jones, B. Gibbons, A. J. Morris, J. R. Morris, D. Troya, *ACS Appl. Mater. Interfaces* **2022**, *14*, 8322–8332.
[31] J. Urzay, *Annu. Rev. Fluid Mech.* **2018**, *50*, 593–627.
[32] P. H. La Marche, G. R. Walton, E. D. Perry, D. M. Manos, M. Leonard, G. J. Gettelfinger, H. F. Dylla, H. L. Bush, in *Fusion Technology 1990* (Eds.: B. E. Keen, M. Huguet, R. Hemsworth), Elsevier, Oxford, **1991**, pp. 341–345.
[33] Y. Wang, E. Hagen, P. Biswas, H. Wang, M. Zachariah, *Combust. Flame* **2023**, *252*, 112747.
[34] M. J. Spalding, H. Krier, R. L. Burton, *Combust. Flame* **2000**, *120*, 200–210.
[35] J. Faridi, M. EL. Guendouzi, *MATEC Web of Conferences* **2013**, *5*, 04002.
[36] Z. Łodziana, P. Błoński, Y. Yan, D. Rentsch, A. Remhof, *J. Phys. Chem. C* **2014**, *118*, 6594–6603.
[37] J. Yang, A. Zheng, M. Zhang, Q. Luo, Y. Yue, C. Ye, X. Lu, F. Deng, *J. Phys. Chem. B* **2005**, *109*, 13124–13131.
[38] J. Wang, T. Steenhaut, H.-W. Li, Y. Filinchuk, *Inorg. Chem.* **2023**, *62*, 2153–2160.
[39] S.-J. Hwang, R. C. Bowman, J. W. Reiter, Rijssenbeek, G. L. Soloveichik, J.-C. Zhao, H. Kabbour, C. C. Ahn, *J. Phys. Chem. C* **2008**, *112*, 3164–3169.
[40] X. Zheng, Y. Yang, F. Zhao, F. Fang, Y. Guo, *Chem. Commun.* **2017**, *53*, 11083–11086.
[41] V. I. Saldin, V. V. Sukhovey, N. N. Savchenko, A. B. Slobodyuk, L. N. Ignatieva, *Russian Journal of Inorganic Chemistry* **2016**, *61*, 630–637.
[42] M. Chrenková, V. Danielik, A. Silný, V. Daněk, *Chem. Pap.* **2001**, *55*, 75–80.
[43] L. He, H.-W. Li, E. Akiba, *Energies* **2015**, *8*, 12429–12438.
[44] E. A. Il'inchik, *J. Appl. Spectrosc.* **2008**, *75*, 883–891.
[45] A. Foelske-Schmitz, D. Weingarth, R. Kötz, *Surf. Sci.* **2011**, *605*, 1979–1985.
[46] L. Caracciolo, L. Madec, H. Martinez, *ACS Appl. Energ. Mater.* **2021**, *4*, 11693–11699.
[47] Y. Ohkubo, Y. Okazaki, M. Nishino, Y. Seto, K. Endo, K. Yamamura, *RSC Adv.* **2022**, *12*, 31246–31254.
[48] M. W. Herdiech, H. Mönig, E. I. Altman, *Surf. Sci.* **2014**, *626*, 53–60.
[49] **N. d**, DOI https://dx.doi.org/10.18434/T4T88K.
[50] M. Khandelwal, G. Pemawat, R. Kanwar Khangarot, *Asian J. Org. Chem.* **2022**, *11*, e202200325.
[51] A. Vodacek, R. L. Kremens, A. J. Fordham, S. C. Vangorden, D. Luisi, J. R. Schott, D. J. Latham, *International Journal of Remote Sensing* **2002**, *23*, 2721–2726.
[52] D. P. Chong, C. Kirby, W. M. Lau, T. Minato, N. P. C. Westwood, *Chem. Phys.* **1981**, *59*, 75–83.
[53] Q. Lai, M. Paskevicius, D. A. Sheppard, C. E. Buckley, A. W. Thornton, M. R. Hill, Q. Gu, J. Mao, Z. Huang, H. K. Liu, Z. Guo, A. Banerjee, S. Chakraborty, R. Ahuja, K.-F. Aguey-Zinsou, *ChemSusChem* **2015**, *8*, 2789–2825.
[54] R. C. Pierce, R. F. Porter, *Inorg. Chem.* **1975**, *14*, 1087–1093.

Manuscript received: January 24, 2024
Accepted manuscript online: June 4, 2024
Version of record online: October 8, 2024